Epithelial-Mesenchymal Transition-Like Phenotypic Changes of Retinal Pigment Epithelium Induced by TGF-β Are Prevented by PPAR-γ Agonists

Hiroki Hatanaka,[1] *Noriko Koizumi,*[2] *Naoki Okumura,*[1,2] *EunDuck P. Kay,*[2,3] *Eri Mizuhara,*[2] *Junji Hamuro,*[1] *and Shigeru Kinoshita*[1]

Purpose. Proliferative eye diseases, such as proliferative vitreoretinopathy and proliferative diabetic retinopathy, are caused partly by fibrotic change of retinal pigment epithelial cells (RPECs). The purpose of our study was to examine the effect of the peroxisome proliferator-activated receptor-γ (PPAR-γ) agonist on the fibrotic change of primate RPECs.

Methods. Monkey RPECs (MRPECs) isolated from a cynomolgus monkey eye were subcultured. To induce fibrotic change, MRPECs were cultured with TGF-β2 (3 ng/mL), and also cultured in the coexistence of TGF-β2 and the PPAR-γ agonist pioglitazone (30 μM). The phenotype of the cultured MRPECs was evaluated by phase contrast microscopy and immunocytochemical analysis. The phosphorylation of Smad2/Smad3 proteins was examined by Western blot analysis.

Results. Primary MRPECs were cultured as a monolayer with a hexagonal cell shape, and positive expression of ZO-1, Na^+/K^+-ATPase, and RPE65 was confirmed. Cell morphology and the expression of these markers were maintained in the presence of pioglitazone, whereas the cells were elongated and the expression of these markers was reduced in its absence. Conversely, the expression of phalloidin, α-smooth muscle actin, and fibronectin was reduced in the presence of pioglitazone, whereas it was increased in the absence. Western blot assay demonstrated that phosphorylation of Smad2/Smad3 proteins was suppressed by pioglitazone.

Conclusions. The PPAR-γ agonist pioglitazone inhibited the fibrotic change of primary MRPECs through the suppression of TGF-β signaling. Pioglitazone might prove to be a clinically applicable and effective pharmaceutic treatment for proliferative eye diseases. (*Invest Ophthalmol Vis Sci.* 2012;53:6955-6963) DOI:10.1167/iovs.12-10488

Intraocular proliferative diseases, such as proliferative vitreoretinopathy (PVR) and proliferative diabetic retinopathy (PDR), are the major cause of vision loss and have poor visual prognosis in spite of the development of innovative surgical techniques and anti-VEGF agents.[1,2] Despite the vigorous accumulation of knowledge about the pathology of PVR over the past decade, little progress has been made toward the clinical management of the disease.[2] To date, to our knowledge no practical pharmacologic treatment has been developed to repair the damaged fibrotic tissues involved in these diseases.

Intraocular fibrosis is a clinically-recognized, underlying pathologic feature in PVR and PDR that leads to functional impairment of the retina. The fibrotic change involves sub- and preretinal fibrosis, scarring, and proliferative membrane. These fibrotic features result in the recurrence of the disease and aggravate the prognosis of visual acuity.[3,4] Such tissue fibrosis also is found in a variety of tissues, such as those of the kidney, liver, lung, and so forth. The fibrous tissue reduces the flexibility of the detached retina and becomes a major cause for failure of retinal reattachment surgery. Once fibrosis occurs, a surgical operation thus far has been the only possible therapeutic modality. In the pathogenesis of PVR and PDR, changes such as proliferation and production of the fibrillar extracellular matrix (ECM) on the retina, occur frequently in retinal pigment epithelial cells (RPECs) located in the vitreous cavity and subretinal space.[2,5] Thus, agents capable of preventing the fibrotic change of RPECs may be of great therapeutic value in retinal reattachment surgery. Numerous drugs have been tested on animal models or cell cultures to inhibit cell proliferation and proliferative membrane formation. However, many of these drugs cause severe side effects and only a few have been used in clinical trials.[2,6]

The epithelial mesenchymal transition (EMT) or transdifferentiation of epithelial cells has been theorized to have a critical role in the development of such pathologic fibrosis.[7-10] In fact, TGF-β signaling has been shown to have a crucial role in these fibrotic changes.[11,12] Recently, numerous reports have demonstrated that treatment with a peroxisome proliferator-activated receptor-γ (PPAR-γ) agonist attenuates experimentally-induced kidney,[13,14] liver,[15] lung,[16] skin,[17] and cardiac fibrosis.[18] In a variety of renal diseases, overexpression of TGF-β isoforms is observed in animals and humans.[19-22] These reports also showed that the PPAR-γ agonist inhibited the fibrotic change by down-regulating the TGF-β pathway.

Likewise, the overexpression of TGF-β has been observed in the vitreous body in PDR and PVR,[23,24] and also has been investigated in relation to the proliferative membranes in these diseases.[25] The purpose of our study was to investigate if a human RPE cell line and primate RPECs exhibited fibrotic changes by TGF-β2, and if PPAR-γ agonists could prevent this fibrotic process. Our findings demonstrated that

From the [1]Department of Ophthalmology, Kyoto Prefectural University of Medicine, Kyoto, Japan; the [2]Department of Biomedical Engineering, Faculty of Life and Medical Sciences, Doshisha University, Kyotanabe, Japan; and the [3]University of Southern California, Los Angeles, California.

The authors alone are responsible for the content and writing of the paper.

Submitted for publication June 28, 2012; revised August 20 and August 31, 2012; accepted August 31, 2012.

Disclosure: **H. Hatanaka**, None; **N. Koizumi**, None; **N. Okumura**, None; **E.P. Kay**, None; **E. Mizuhara**, None; **J. Hamuro**, None; **S. Kinoshita**, None

Corresponding author: Noriko Koizumi, Department of Biomedical Engineering, Faculty of Life and Medical Sciences, Doshisha University, Kyotanabe 610-0321, Japan; nkoizumi@mail.doshisha.ac.jp.

the PPAR-γ agonist restored the fibrotic pathologic changes mediated by TGF-β2.

METHODS

Materials

For our study, recombinant human TGF-β2 was purchased from R&D Systems, Inc. (Minneapolis, MN). Pioglitazone was purchased from Enzo Life Sciences, Inc. (Farmingdale, NY). Dulbecco's modified Eagle medium:Nutrient Mixture (DMEM/F12), penicillin, streptomycin, Alexa Fluor 546 phalloidin, Alexa Fluor 488 donkey anti-mouse IgG, and Alexa Fluor 594 donkey anti-rabbit IgG were purchased from Life Technologies Corporation (Carlsbad, CA). Dispase II was purchased from Roche Applied Science (Penzberg, Germany), and FNC Coating Mix was purchased from Athena Environmental Sciences, Inc. (Baltimore, MD). ZO-1 polyclonal antibody was purchased from Zymed Laboratories, Inc. (South San Francisco, CA), Na^+-K^+-ATPase monoclonal antibody was purchased from Upstate Biotechnology, Inc. (Lake Placid, NY), and DAPI was purchased from Vector Laboratories, Inc. (Burlingame, CA). N-cadherin and fibronectin antibody were purchased from BD Biosciences Pharmingen (Franklin Lakes, NJ). Smad-2, Smad3, and phosphorylated Smad2 (phospho-Smad2) and phosphor-Smad3 antibody were purchased from Cell Signaling Technology, Inc. (Danvers, MA). Alpha smooth muscle (αSMA) antibody was purchased from Thermo Fisher Scientific, Inc. (Waltham, MA). RPE65 antibody and GAPDH were purchased from Abcam, Inc. (Cambridge, MA). Phosphatase inhibitor was purchased from Sigma-Aldrich Corporation (St. Louis, MO).

Animal Experiment Approval

In all experiments, animals were housed and treated in accordance with the ARVO Statement for the Use of Animals in Ophthalmic and Vision Research.

Cell Culture and Treatment of ARPE-19

ARPE-19, a human RPE cell line, was purchased from the American Type Culture Collection (ATCC; Manassas, VA). The cells were cultured in DMEM/F12 supplemented with 10% fetal bovine serum (FBS), 50 U/mL penicillin, and 50 μg/mL streptomycin in a humidified atmosphere at 37°C in 5% CO_2 for more expansion.[26] As described previously, the cells were treated in the fresh medium with recombinant human TGF-β2 (5 ng/mL, fibrotic group) or serum-free medium (control group) after 24 hours of serum starvation when the cells reached confluency.[27] Next, we investigated if a difference could be found between the control and fibrotic groups in the morphology of ARPE-19. The ratio of elongated cells cultured under various conditions then was calculated. The elongated cells were defined as ones in which the length of the cell is two times longer than the width of that cell. ARPE-19 cells were seeded at a density of 1.0×10^5 cells onto 12-well plates in the medium containing 10% FBS. PPAR-γ agonist was added at the concentration of 10 and 30 μM with TGF-β2 (PPAR-γ group) simultaneously.

Cell Culture and Treatment of Monkey RPECs (MRPECs)

MRPECs were cultured from the posterior area of an eyeball enucleated from a cynomolgus monkey (3–5 years old, estimated equivalent human age 5–20 years) housed at Nissei Bilis Co., Ltd. (Otsu, Japan). The MRPECs then were separated from the RPEC fragments in accordance with the method described previously for human fetal RPE.[28] The MRPECs then were cultured on FNC Coating Mix-coated dishes in DMEM/F12 supplemented with 10% FBS, 50 U/mL of penicillin, and 50 μg/mL of streptomycin for more expansion in a humidified atmosphere at 37°C in 5% CO_2. The culture medium then was changed every 2 days. When the cells reached confluency in 5 to 7 days, they were rinsed in Ca^{2+} and Mg^{2+}-free Dulbecco's phosphate-buffered saline (PBS), trypsinized with 0.05% Trypsin-EDTA (Life Technologies) for 5 minutes at 37°C, and passaged at ratios of 1:2 to 4. Cultivated MRPECs at passages 1 to 3 were used for all experiments. MRPECs then were treated with recombinant human TGF-β2 (3 ng/mL) (fibrotic group) or 2% FBS-containing medium (control) after 24 hours of serum starvation when the cells reached confluency. As a PPAR-γ group, MRPECs were cultured with medium containing TGF-β2 and PPAR-γ agonist (30 μM). The morphologic differences among the groups then were observed. The MRPECs then were seeded at a density of 1.0×10^5 cells onto 24-well plates in the medium containing 10% FBS to investigate if a difference in cell morphology could be found among the groups.

Immunocytochemistry

To analyze the expression and localization of function-related proteins in the cells, ARPE-19 cells and MRPECs were cultured at a density of 3×10^4 cells/cm^2 on Lab-Tek Chamber Slides (NUNC A/S, Roskilde, Denmark) in various conditions for 48 hours before staining. The cells then were stained with individual antibodies; namely, anti-ZO-1, anti-Na^+/K^+-ATPase, anti-RPE65, anti-N cadherin, anti-E cadherin, anti-phalloidin, anti-fibronectin, and anti-α smooth muscle antibodies. For a second antibody, 1:2000 diluted Alexa Fluor 488 donkey anti-mouse IgG and 1:2000 diluted Alexa Fluor 594 donkey anti-rabbit IgG were used. Cell nuclei then were stained with DAPI, and the slides were inspected by use of a fluorescence microscope.

Reverse Transcriptase-Polymerase Chain Reaction (RT-PCR)

For RT-PCR, total RNA was extracted by use of TRIzol reagent (Life Technologies) and treated with RNase-free DNase I (Roche). cDNA was synthesized with SuperScript III Reverse Transcriptase (Life Technologies) and PCR reactions then were performed with EX Taq DNA polymerase (Takara Bio, Shiga, Japen) as follows: denaturation at 94°C for 30 seconds, 23 to 35 cycles of annealing at 55°C to 57°C for 30 seconds, and elongation at 72°C for 30 seconds. The PCR products then were separated by electrophoresis on 2% agarose gels and detected under ultraviolet illumination.

Real-Time Quantitative PCR (qPCR)

For the real-time qPCR, reverse transcription was conducted using the TaqMan Fast Advanced Master Mix (Applied Biosystems, Inc., Foster City, CA) according to the manufacturer's protocol. Real-time qPCR reactions then were conducted by use of the StepOnePlus (Applied Biosystems) real-time PCR system according to the manufacturer's protocol.

Western Blot Analysis

For the detection of Smad2, Smad3, phospho-Smad2, and phospho-Smad3, MRPECs were serum-starved for 24 hours and then incubated with TGF-β2, or TGF-β2 and PPAR-γ agonist-containing medium for 10 minutes and extracted with Tris-buffered saline containing phosphatase inhibitors. The proteins then were separated by use of SDS-PAGE and transferred to a polyvinylidene fluoride membrane. The blots were blocked overnight with nonfat dried milk and incubated with rabbit anti-human phospho-Smad2 monoclonal antibody, rabbit anti-human phospho-Smad3 monoclonal antibody, rabbit anti-human Smad2, or rabbit anti-human Smad3. Luminescence was observed by use of an ImageQuant LAS-4000

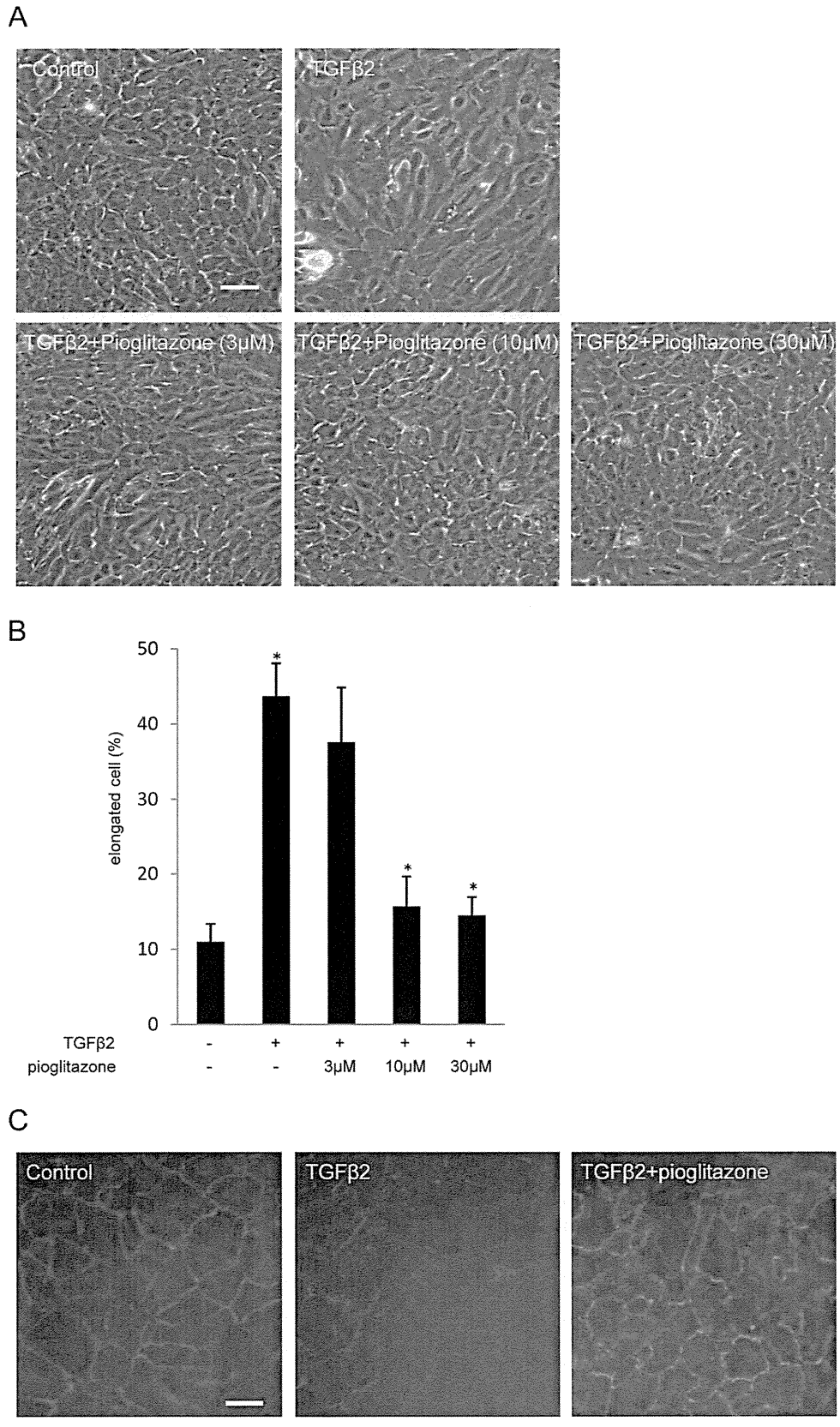

Figure 1. Fibrotic change induced by TGF-β2 and the inhibitory effect of pioglitazone on the morphologic change in ARPE-19 cells. Phase-contrast light microscope images of ARPE-19 cells with TGF-β2 (5 ng/mL) and pioglitazone (3, 10, 30 μM; [**A**]), the ratio of elongated cells in each condition (i.e., the control, TGFβ and PPAR-γ conditions; [**B**]; $n = 4$; $P < 0.005$), and immunocytochemical staining of ZO-1 (**C**) are shown. *Scale bar*: 100 μm.

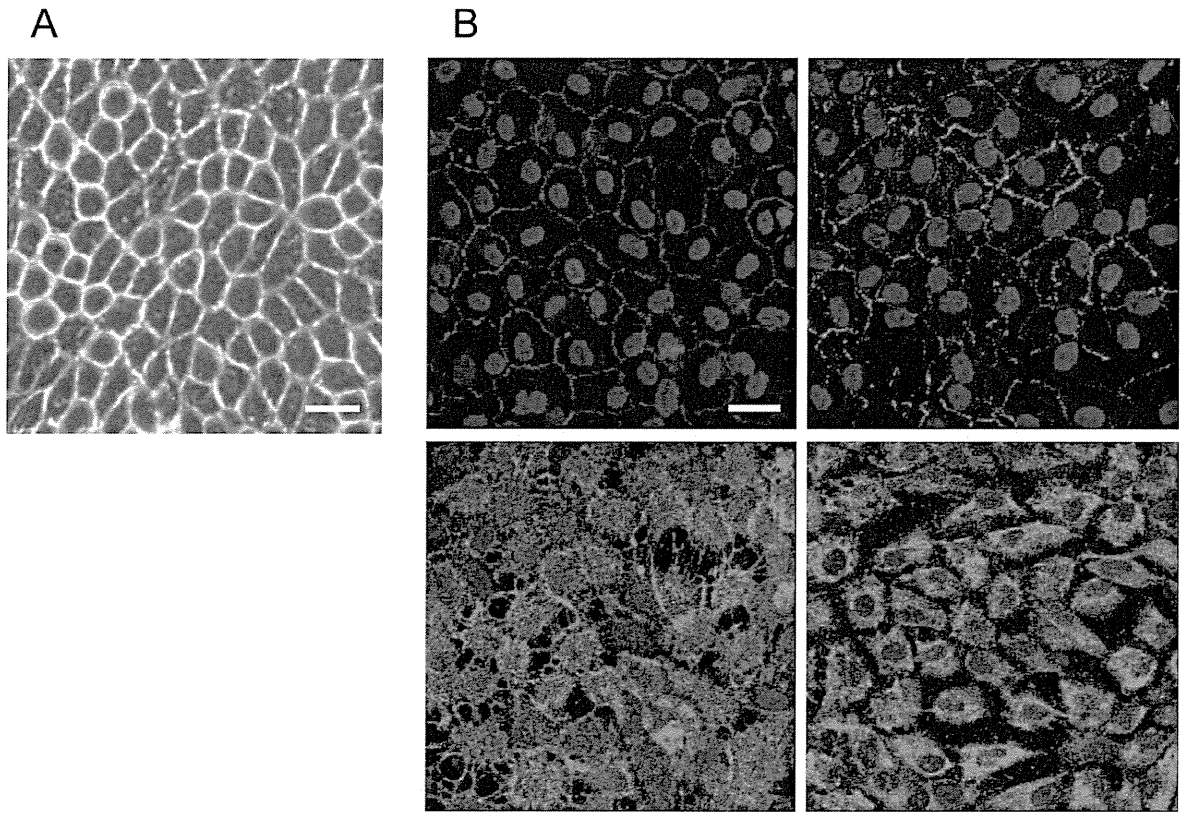

FIGURE 2. Images of primary MRPECs ($P = 1$) immunocytochemically stained (**A**) with ZO-1 (*top left*), N-cadherin (*top right, green*), Na^+/K^+-ATPase (*bottom left*), RPE65 (*bottom right, green*), and a phase-contrast light microscopy image (**B**). *Scale bar*: 100 μm.

mini (FUJIFILM, Tokyo, Japan) dedicated charge-coupled device (CCD) camera system.[29]

RESULTS

Preventive Effect of PPAR-γ Agonist against the TGF-β2–Induced Morphologic Change in ARPE-19

The cellular morphology of ARPE-19 cells is the characteristic cuboidal shape under normal culture conditions. On the other hand, the presence of TGF-β2 (5 ng/mL) induced an EMT-like morphologic change of ARPE-19 cells, symbolized by the elongated and fibroblastic phenotypes (Fig. 1A). TGF-β2 at 5 ng/mL, a concentration that is nontoxic and is known to be the most effective, was used in the following experiments. When cells were treated simultaneously with TGF-β2 and PPAR-γ agonist (pioglitazone), pioglitazone at 3 μM demonstrated a mixture of cuboidal and elongated cell shapes, while pioglitazone at 10 and 30 μM reversed the fibroblastic cell shape mediated by TGF-β2 to the cuboidal cell shape. Those results indicated that the PPAR-γ agonist has a concentration-dependent preventive effect against the fibrotic or EMT-like phenotypic change of ARPE-19 cells induced by TGF-β2 (Fig. 1B). The preventive effect of pioglitazone toward the TGF-β2-mediated phenotypic changes of ARPE-19 was confirmed further by use of ZO-1, one of the major epithelial functional tight junction molecules. The immunostaining of ARPE-19 cells with ZO-1 antibody showed the characteristic staining pattern of ZO-1 at the plasma membrane, while cells treated with TGF-β2 greatly reduced the ZO-1 staining potential. On the other hand, cells treated with TGF-β2 and pioglitazone demonstrated the cuboidal cell shape with the distinct ZO-1 staining pattern (Fig. 1C).

Influence of PPAR-γ Agonist and TGF-β2 on the Expression of Functional Molecules in MRPECs

The established MRPEC cultures were maintained in DMEM/F12 medium containing 2% FBS, a concentration that minimizes the TGF-β activity of FBS, and the MRPECs demonstrated the characteristic hexagonal or polygonal morphology (Fig. 2A). That culture condition also maintained the expression of functional proteins, such as ZO-1, Na^+/K^+-ATPase, N-cadherin, and RPE65 (an essential protein for the visual cycle), and the proteins were expressed according to their subcellular localization (Fig. 2B).

When MRPECs were treated with TGF-β2, they lost their characteristic polygonal cell morphology. However, simultaneous treatment of the cells with TGF-β2 and pioglitazone reversed the cell shape change induced by TGF-β2 (Fig. 3A). Those results indicated the induction of the EMT-like or fibrotic change of MRPECs by TGF-β2 (Fig. 3A). TGF-β2 (3 ng/mL) was chosen as the optimal concentration for the induction of the fibrotic change of the MRPECs. The morphologic changes of the MRPECs induced by TGF-β2 (the EMT-like or fibrotic change) were reduced in the presence of pioglitazone below those in the TGF-β2 group.

The changes of distribution of ZO-1 (Fig. 3B), Na^+/K^+-ATPase (Fig. 3C), and N-cadherin (Fig. 3D) in the MRPECs were observed in the TGF-β2–treated group when compared to those of control cells. However, the TGF-β2 changes were inhibited by the PPAR-γ agonist pioglitazone (Figs. 3B, 3C, 3D). The expression of RPE65 and N-cadherin was examined further by use of real-time qPCR, which showed that the RPE65 expression was reduced markedly by TGF-β2, while the N-cadherin mRNA was increased by TGF-β2. Of interest, pioglitazone blocked such TGF-β2–mediated changes (Fig. 3E). The same tendency was observed in N-cadherin mRNA expressions using real-time PCR (Fig. 3F).

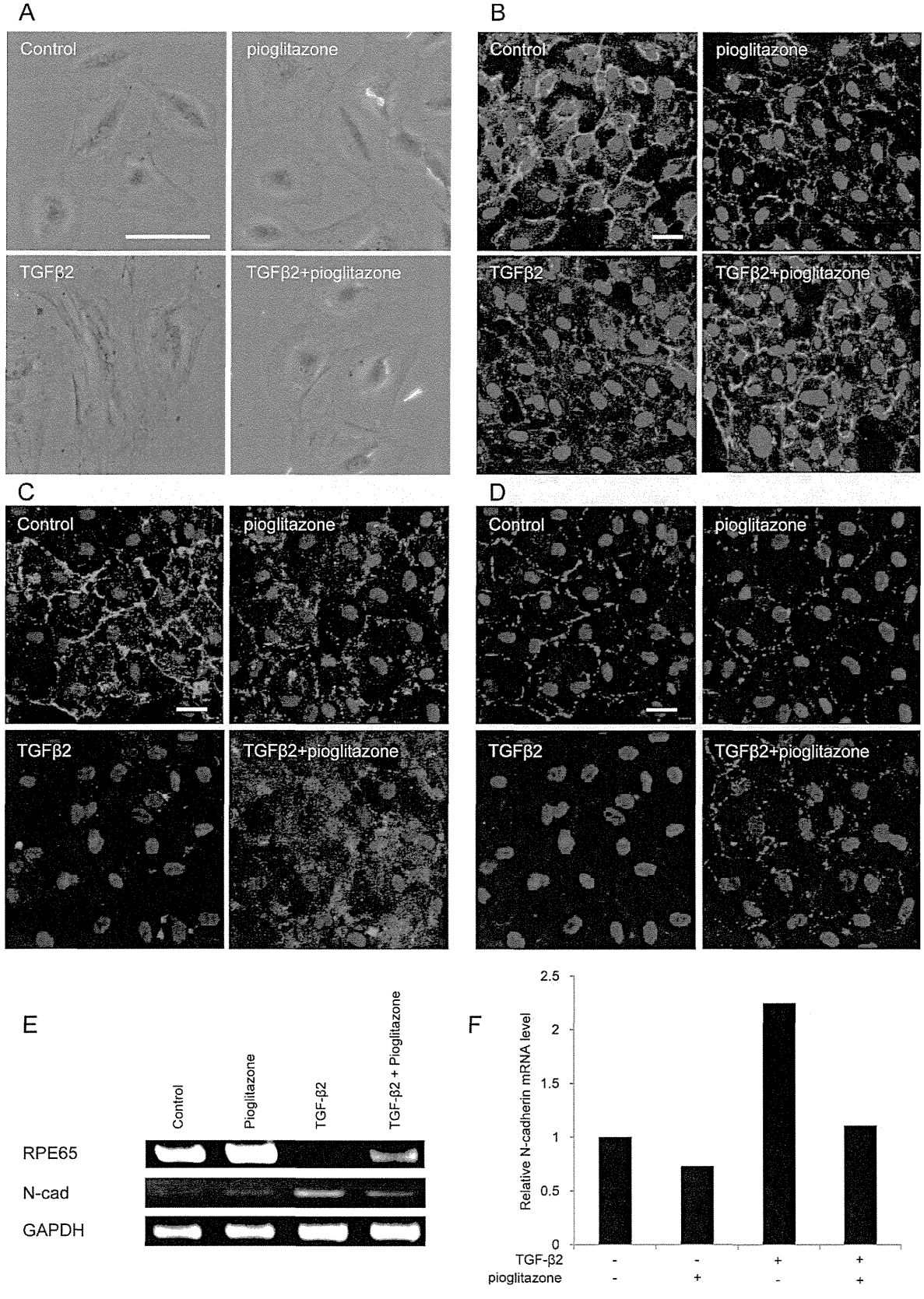

Figure 3. The effect of pioglitazone on fibrotic change induced by TGF-β2 in primary MRPECs. Phase-contrast light microscopy images of primary MRPECs (**A**), and the change of distribution in the expression of N-cadherin (**B**), Na^+/K^+-ATPase (**C**), and ZO-1 (**D**) in the medium with TGF-β2 (3 ng/mL) and/or pioglitazone (30 μM). (**E**) An image showing the mRNA expression of RPE65 and N-cadherin. (**F**) An image showing the ratio of the expression of N-cadherin mRNA as compared to the control. *Scale bar*: 100 μm.

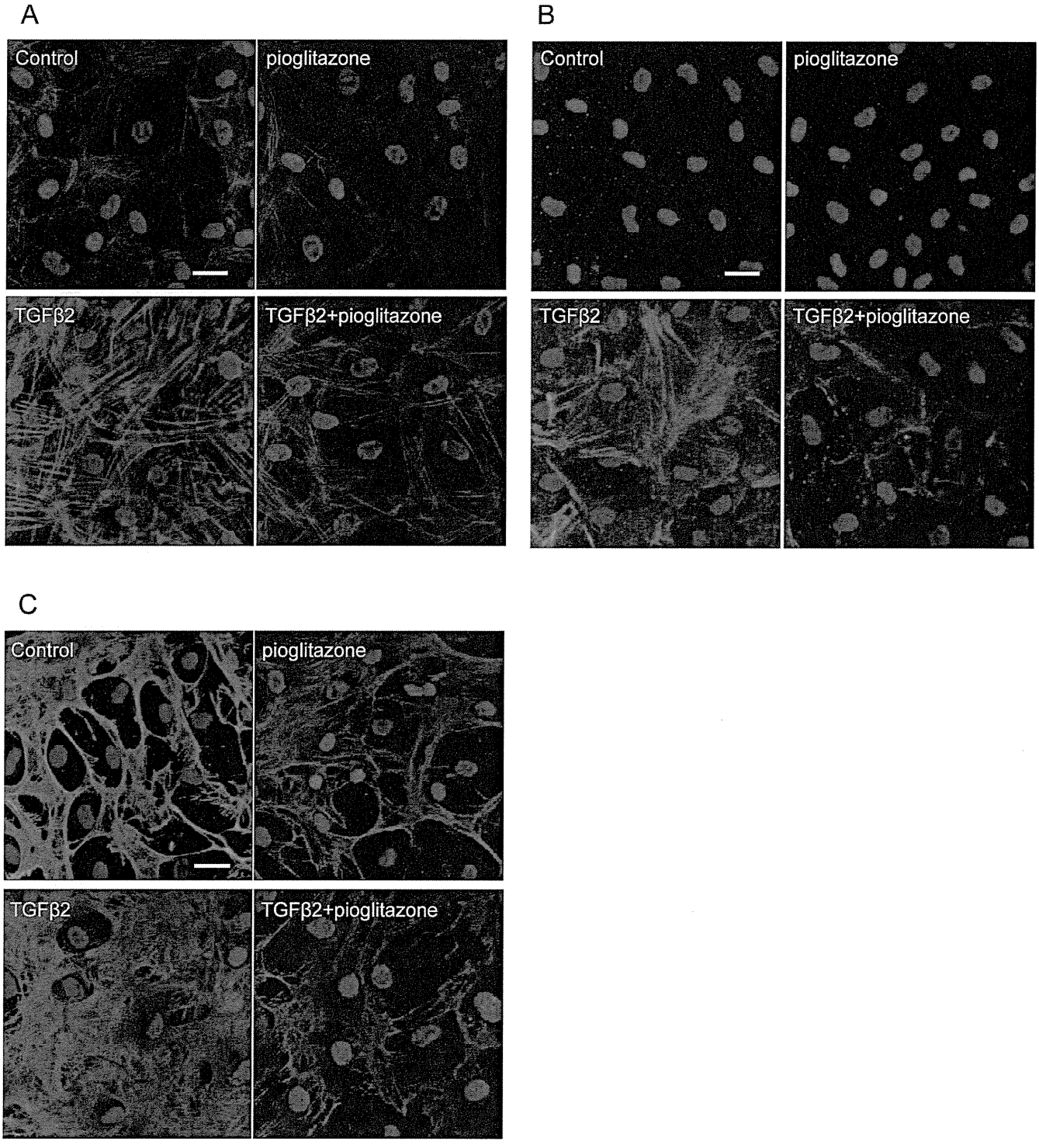

FIGURE 4. The effect of pioglitazone and TGF-β2 on the cytoskeleton of MRPECs. Images showing the immunostaining of phalloidin (**A**), αSMA (**B**), and fibronectin (**C**). *Scale bar*: 100 μm.

Next, the expression of fibrotic or EMT-related markers, such as stress fibers (Fig. 4A), α-smooth muscle actin (α-SMA, Fig. 4B), and fibronectin (Fig. 4C) was determined. The control cells demonstrated a low level of these EMT-related markers. However, the expression of these proteins was increased by exposure to TGF-β2 and that increase was reversed almost to normal control levels by the addition of PPAR-γ agonist pioglitazone.

Effect of PPAR-γ Agonist and TGF-β2 on the Smad Pathway in MRPECs

Finally, we investigated if the Smad pathway was related to the aforementioned findings. The expression of phospho-Smad2 and phospho-Smad3 proteins was detected only faintly in the control cells (Figs. 5A, 5B); however, phosphorylation of

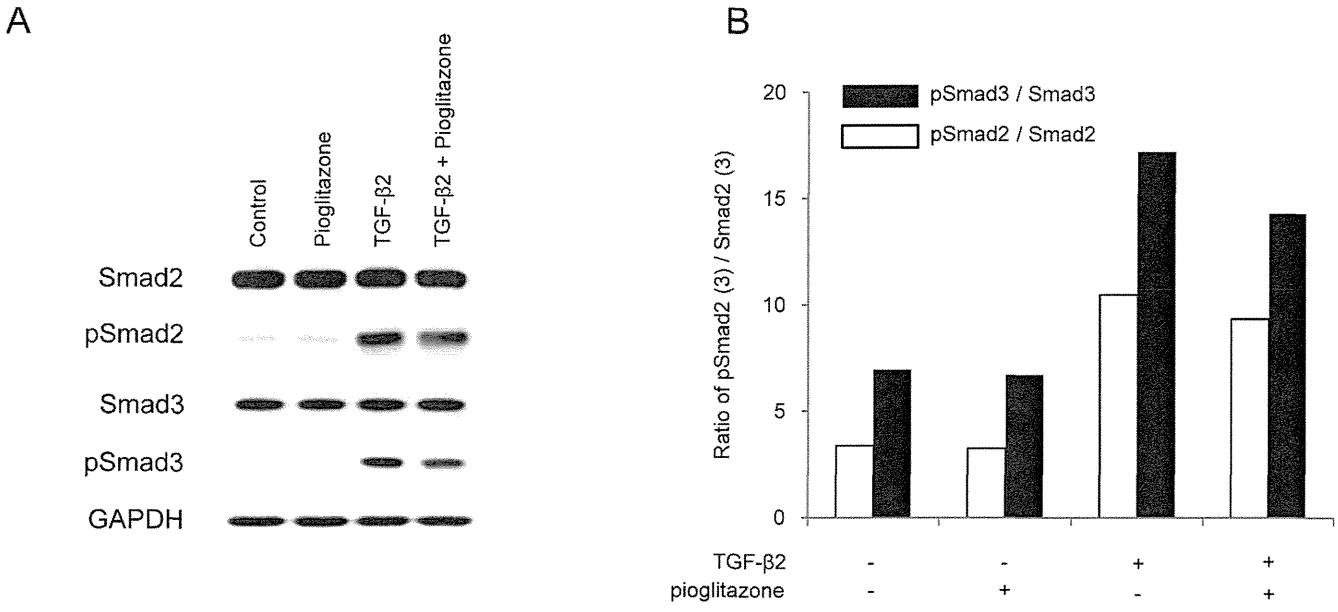

Figure 5. (**A**) The expressions of Smad2, phospho-Smad2 (pSmad2), Smad3, and pSmad3 after exposure to TGF-β2 and/or pioglitazone for 10 minutes. (**B**) The representative result is shown. Protein accumulation was assessed by densitometry ($n = 3$).

Smad2 and Smad3 was increased greatly in response to TGF-β2 stimulation (Figs. 5A, 5B). The PPAR-γ agonist tended to inhibit the phosphorylation of Smad2 and Smad3, yet at a low level (Fig. 5B).

Discussion

Intraocular fibrosis within a proliferative membrane is a clinically recognized underlying pathologic feature in PVR and PDR that leads to functional impairment of the retina. The proliferative membrane reportedly contains RPECs, hyalocytes, glial cells, and macrophage-derived cells,[30] and RPECs are known to have a key role in developing pathology. Numerous studies have reported the fibrotic- or EMT-like change by use of the ARPE-19 cell line, a human RPE cell line. Nonetheless, the established cell lines may have an intrinsic weakness, such as obtaining an abnormal chromosome along with passages. Thus, test results obtained through the use of these cells might not precisely mimic those of human primary cells. This concern led us to establish primate primary RPECs, similar to human primary RPECs.

TGF-β2[31] and vitreous specimens obtained from PVR or PDR[32] have been used to induce fibrotic change in ARPR-19 cells. The increased concentration of TGF-β2 in intraocular proliferative diseases is well known,[23] thus prompting us to investigate TGF-β2 as an inducer of fibrotic phase transition in our primate primary RPEC model. Fibrotic change of the primary MRPECs was observed as the accumulation of actin filaments in the cytoplasm. Overexpression of αSMA and fibronectin was detected, suggesting that TGF-β2 induces EMT-like phenotypic changes in the primary MRPECs similar to that in the human RPE cell line. These ECM proteins, major components of the proliferative membrane, are the typical pathologic features evident in intraocular proliferative diseases. Furthermore, expression of functional proteins, such as ZO-1, Na^+/K^+-ATPase, N-cadherin, and RPE65, was diminished at the cell surface in response to TGF-β2 stimulation. These findings suggested that we successfully made an in vitro model of an intraocular proliferative disease using primary MRPECs, and that RPECs lost the characteristic epithelial phenotypes and assumed EMT-like phenotypic changes by TGF-β2.

We further investigated the preventive effect of pioglitazone on the fibrotic- or EMT-like change induced by TGF-β2. A recent study showed that troglitazone, one of the PPAR-γ agonists, can prevent TGF-β2–induced EMT-like changes in the human RPE cell line.[33] Our results with pioglitazone, another PPAR-γ agonist, are consistent with the observation obtained from the human RPE cell line treated with troglitazone. The inhibitory effect of pioglitazone on EMT reportedly also has been observed in corneal keratocytes,[34] kidney cells,[14] and lung cells.[16] Importantly, our findings demonstrated the preventive effect of the PPAR-γ agonist pioglitazone on EMT by use of primary MRPECs. In this investigation, it is not uncovered if the effects of pioglitazone on the TGF-β2–induced EMT in cells are attributable to the PPAR-γ receptor-involved mechanism. Some of the glitazone members exhibit anti-TGF-β effects through non-PPAR-γ signaling. Thus, it is necessary to test whether or not the action reported here is via PPAR-γ. We currently are planning a future study to elucidate the molecular mechanism of the pioglitazone-mediated anti-EMT phenomenon in RPE cells, for example by using a dominant negative PPAR-γ system. The aim of our present study was to clarify the effect of PPAR-γ on the cynomolgus monkey primary RPE cells, instead of the long-term maintained cell lines. For the PPAR-γ overexpression system, it usually is necessary to use stable cell lines to investigate the intracellular events.

EMT can be induced or regulated by various growth and differentiation factors, including TGF-β, fibroblast growth factor, hepatic growth factor, and Wnt and Notch proteins.[35] Intracellular signaling molecules, such as p38 MAP kinase,[36] Notch,[37] Wnt,[38] NF-κB,[39] and phosphatidylinositol-3-OH kinase,[40] also reportedly are involved in the TGF-β signaling pathway. In the Smad pathway, after TGF-β binds to the receptor, the complex of phosphorylated Smad2/3 and Smad4 is translocated into the cell nucleus following gene overexpression in genes, such as *COL1A1*.[41] Of interest, our findings demonstrated that pioglitazone hampers phosphorylation of Smad2/3 activated by TGF-β2 in primate primary RPECs, yet at a low level. However, the precise mechanism by which pioglitazone induces the suppression of EMT in primate primary RPECs has yet to be elucidated.

The findings of our present study demonstrated that pioglitazone, a drug now being used for the treatment of diabetes mellitus, may hold the potential of being a clinically applicable pharmaceutic agent for the prevention or inhibition of intraocular proliferative diseases in the early stage of the pathology or if applied following surgery for retinal detachment. Further investigation using PVR, PDR, and AMD in vivo models is crucial to elucidate the pathology of these diseases and to discover clinically applicable therapeutic interventions for these diseases. Such future investigations hopefully will lead to the development of new drugs, such as pioglitazone.

Acknowledgments

Yuji Sakamoto provided the monkey eyeball used in this study and John Bush reviewed the manuscript.

References

1. Fong DS, Aiello L, Gardner TW, et al. Diabetic retinopathy. *Diabetes Care*. 2003;26(suppl 1):S99-S102.
2. Pastor JC, de la Rua ER, Martin F. Proliferative vitreoretinopathy: risk factors and pathobiology. *Prog Retin Eye Res*. 2002; 21:127-144.
3. Richter-Mueksch S, Stur M, Stifter E, Radner W. Differences in reading performance of patients with drusen maculopathy and subretinal fibrosis after CNV. *Graefes Arch Clin Exp Ophthalmol*. 2006;244:154-162.
4. Unver YB, Yavuz GA, Bekiroglu N, Presti P, Li W, Sinclair SH. Relationships between clinical measures of visual function and anatomic changes associated with bevacizumab treatment for choroidal neovascularization in age-related macular degeneration. *Eye (Lond)*. 2009;23:453-460.
5. Antonetti DA, Klein R, Gardner TW. Diabetic retinopathy. *N Engl J Med*. 2012;366:1227-1239.
6. Pastor JC. Proliferative vitreoretinopathy: an overview. *Surv Ophthalmol*. 1998;43:3-18.
7. Iwano M, Plieth D, Danoff TM, Xue C, Okada H, Neilson EG. Evidence that fibroblasts derive from epithelium during tissue fibrosis. *J Clin Invest*. 2002;110:341-350.
8. Schnaper HW, Hayashida T, Hubchak SC, Poncelet AC. TGF-beta signal transduction and mesangial cell fibrogenesis. *Am J Physiol Renal Physiol*. 2003;284:F243-F252.
9. Willis BC, Borok Z. TGF-beta-induced EMT: mechanisms and implications for fibrotic lung disease. *Am J Physiol Lung Cell Mol Physiol*. 2007;293:L525-L534.
10. Gressner AM, Weiskirchen R, Breitkopf K, Dooley S. Roles of TGF-beta in hepatic fibrosis. *Front Biosci*. 2002;7:d793-d807.
11. Piek E, Moustakas A, Kurisaki A, Heldin CH, ten Dijke P. TGF-(beta) type I receptor/ALK-5 and Smad proteins mediate epithelial to mesenchymal transdifferentiation in NMuMG breast epithelial cells. *J Cell Sci*. 1999;112(Pt 24):4557-4568.
12. Valcourt U, Kowanetz M, Niimi H, Heldin CH, Moustakas A. TGF-beta and the Smad signaling pathway support transcriptomic reprogramming during epithelial-mesenchymal cell transition. *Mol Biol Cell*. 2005;16:1987-2002.
13. Kawai T, Masaki T, Doi S, et al. PPAR-gamma agonist attenuates renal interstitial fibrosis and inflammation through reduction of TGF-beta. *Lab Invest*. 2009;89:47-58.
14. Higashi K, Oda T, Kushiyama T, et al. Additive antifibrotic effects of pioglitazone and candesartan on experimental renal fibrosis in mice. *Nephrology (Carlton)*. 2010;15:327-335.
15. Galli A, Crabb DW, Ceni E, et al. Antidiabetic thiazolidinediones inhibit collagen synthesis and hepatic stellate cell activation in vivo and in vitro. *Gastroenterology*. 2002;122: 1924-1940.
16. Aoki Y, Maeno T, Aoyagi K, et al. Pioglitazone, a peroxisome proliferator-activated receptor gamma ligand, suppresses bleomycin-induced acute lung injury and fibrosis. *Respiration*. 2009;77:311-319.
17. Wu M, Melichian DS, Chang E, Warner-Blankenship M, Ghosh AK, Varga J. Rosiglitazone abrogates bleomycin-induced scleroderma and blocks profibrotic responses through peroxisome proliferator-activated receptor-gamma. *Am J Pathol*. 2009;174:519-533.
18. Shiomi T, Tsutsui H, Hayashidani S, et al. Pioglitazone, a peroxisome proliferator-activated receptor-gamma agonist, attenuates left ventricular remodeling and failure after experimental myocardial infarction. *Circulation*. 2002;106: 3126-3132.
19. Chen S, Jim B, Ziyadeh FN. Diabetic nephropathy and transforming growth factor-beta: transforming our view of glomerulosclerosis and fibrosis build-up. *Semin Nephrol*. 2003;23:532-543.
20. Hills CE, Squires PE. TGF-beta1-induced epithelial-to-mesenchymal transition and therapeutic intervention in diabetic nephropathy. *Am J Nephrol*. 2010;31:68-74.
21. Hill C, Flyvbjerg A, Gronbaek H, et al. The renal expression of transforming growth factor-beta isoforms and their receptors in acute and chronic experimental diabetes in rats. *Endocrinology*. 2000;141:1196-1208.
22. Cheng J, Grande JP. Transforming growth factor-beta signal transduction and progressive renal disease. *Exp Biol Med (Maywood)*. 2002;227:943-956.
23. Connor TB Jr, Roberts AB, Sporn MB, et al. Correlation of fibrosis and transforming growth factor-beta type 2 levels in the eye. *J Clin Invest*. 1989;83:1661-1666.
24. Hirase K, Ikeda T, Sotozono C, Nishida K, Sawa H, Kinoshita S. Transforming growth factor beta2 in the vitreous in proliferative diabetic retinopathy. *Arch Ophthalmol*. 1998;116:738-741.
25. Bochaton-Piallat ML, Kapetanios AD, Donati G, Redard M, Gabbiani G, Pournaras CJ. TGF-beta1, TGF-beta receptor II and ED-A fibronectin expression in myofibroblast of vitreoretinopathy. *Invest Ophthalmol Vis Sci*. 2000;41:2336-2342.
26. Dunn KC, Aotaki-Keen AE, Putkey FR, Hjelmeland LM. ARPE-19, a human retinal pigment epithelial cell line with differentiated properties. *Exp Eye Res*. 1996;62:155-169.
27. Kimoto K, Nakatsuka K, Matsuo N, Yoshioka H. p38 MAPK mediates the expression of type I collagen induced by TGF-beta 2 in human retinal pigment epithelial cells ARPE-19. *Invest Ophthalmol Vis Sci*. 2004;45:2431-2437.
28. Maminishkis A, Chen S, Jalickee S, et al. Confluent monolayers of cultured human fetal retinal pigment epithelium exhibit morphology and physiology of native tissue. *Invest Ophthalmol Vis Sci*. 2006;47:3612-3624.
29. Parapuram SK, Chang B, Li L, et al. Differential effects of TGFbeta and vitreous on the transformation of retinal pigment epithelial cells. *Invest Ophthalmol Vis Sci*. 2009;50:5965-5974.
30. Oberstein SY, Byun J, Herrera D, Chapin EA, Fisher SK, Lewis GP. Cell proliferation in human epiretinal membranes: characterization of cell types and correlation with disease condition and duration. *Mol Vis*. 2011;17:1794-1805.
31. Saika S, Yamanaka O, Ikeda K, et al. Inhibition of p38MAP kinase suppresses fibrotic reaction of retinal pigment epithelial cells. *Lab Invest*. 2005;85:838-850.
32. Casaroli-Marano RP, Pagan R, Vilaro S. Epithelial-mesenchymal transition in proliferative vitreoretinopathy: intermediate filament protein expression in retinal pigment epithelial cells. *Invest Ophthalmol Vis Sci*. 1999;40:2062-2072.
33. Cheng HC, Ho TC, Chen SL, Lai HY, Hong KF, Tsao YP. Troglitazone suppresses transforming growth factor beta-

mediated fibrogenesis in retinal pigment epithelial cells. *Mol Vis*. 2008;14:95–104.

34. Pan H, Chen J, Xu J, Chen M, Ma R. Antifibrotic effect by activation of peroxisome proliferator-activated receptor-gamma in corneal fibroblasts. *Mol Vis*. 2009;15:2279–2286.
35. Moustakas A, Heldin CH. Signaling networks guiding epithelial-mesenchymal transitions during embryogenesis and cancer progression. *Cancer Sci*. 2007;98:1512–1520.
36. Zavadil J, Bottinger EP. TGF-beta and epithelial-to-mesenchymal transitions. *Oncogene*. 2005;24:5764–5774.
37. Zavadil J, Cermak L, Soto-Nieves N, Bottinger EP. Integration of TGF-beta/Smad and Jagged1/Notch signalling in epithelial-to-mesenchymal transition. *EMBO J*. 2004;23:1155–1165.
38. Masszi A, Fan L, Rosivall L, et al. Integrity of cell-cell contacts is a critical regulator of TGF-beta 1-induced epithelial-to-myofibroblast transition: role for beta-catenin. *Am J Pathol*. 2004; 165:1955–1967.
39. Huber MA, Azoitei N, Baumann B, et al. NF-kappaB is essential for epithelial-mesenchymal transition and metastasis in a model of breast cancer progression. *J Clin Invest*. 2004;114: 569–581.
40. Bakin AV, Tomlinson AK, Bhowmick NA, Moses HL, Arteaga CL. Phosphatidylinositol 3-kinase function is required for transforming growth factor beta-mediated epithelial to mesenchymal transition and cell migration. *J Biol Chem*. 2000; 275:36803–36810.
41. Burch ML, Zheng W, Little PJ. Smad linker region phosphorylation in the regulation of extracellular matrix synthesis. *Cell Mol Life Sci*. 2011;68:97–107.

PLOS ONE

HLA-A*0206 with TLR3 Polymorphisms Exerts More than Additive Effects in Stevens-Johnson Syndrome with Severe Ocular Surface Complications

Mayumi Ueta[1,2]*, Katsushi Tokunaga[3], Chie Sotozono[1], Hiromi Sawai[3], Gen Tamiya[4], Tsutomu Inatomi[1], Shigeru Kinoshita[1]

1 Department of Ophthalmology, Kyoto Prefectural University of Medicine, Kyoto, Japan, **2** Research Center for Inflammation and Regenerative Medicine, Faculty of Life and Medical Sciences, Doshisha University, Kyoto, Japan, **3** Department of Human Genetics, Graduate School of Medicine, University of Tokyo, Tokyo, Japan, **4** Advanced Molecular Epidemiology Research Institute, Faculty of Medcine, Yamagata University, Yamagata, Japan

Abstract

Background: Stevens-Johnson syndrome (SJS) is an acute inflammatory vesiculobullous reaction of the skin and mucosa, often including the ocular surface, and toxic epidermal necrolysis (TEN) occurs with its progression. Although SJS/TEN is thought to be initiated by certain types of medication coupled with possible infection. In the present study we examined the multiplicative interaction(s) between HLA-A*0206 and 7 Toll-like receptor 3 (TLR3) Single-nucleotide polymorphisms (SNPs) in patients with SJS/TEN.

Principal Findings: We analyzed the genotypes for HLA-A and 7 TLR3 SNPs in 110 Japanese SJS/TEN patients with severe ocular complications and 206 healthy volunteers to examine the interactions between the two loci. We found that HLA-A*0206 exhibited a high odds ratio for SJS/TEN (carrier frequency: OR = 5.1; gene frequency: OR = 4.0) and that there was a strong association with TLR3 rs.5743312T/T SNP (OR = 7.4), TLR3 rs.3775296T/T SNP (OR = 5.8), TLR3 rs.6822014G/G SNP (OR = 4.8), TLR3 rs.3775290A/A SNP (OR = 2.9), TLR3 rs.7668666A/A SNP (OR = 2.7), TLR3 rs.4861699G/G SNP (OR = 2.3), and TLR3 rs.11732384G/G SNP (OR = 1.9). There was strong linkage disequilibrium (LD) between rs.3775296 and rs.5743312 and between rs.7668666 and rs.3775290. The results of interaction analysis showed that the pair, HLA-A*0206 and TLR3 SNP rs3775296T/T, which exhibited strong LD with TLR3 rs.5743312, exerted more than additive effects (OR = 47.7). The other pairs, HLA-A*0206 and TLR3 rs.3775290A/A SNP (OR = 11.4) which was in strong LD with TLR3 rs7668666A/A SNP, and TLR3 rs4861699G/G SNP (OR = 7.6) revealed additive effects. Moreover, the combination HLA-A*0206 and TLR3 rs3775296T/T was stronger than the TLR3 rs6822014G/G and TLR3 rs3775290A/A pair, which reflected the interactions within the TLR3 gene alone.

Significance: By interaction analysis, HLA-A*0206 and TLR3 SNP rs3775296T/T, which were in strong LD with TLR3 SNP rs5743312T/T, manifested more than additive effects that were stronger than the interactions within the TLR3 gene alone. Therefore, multiplicative interactions of HLA-A and TLR3 gene might be required for the onset of SJS/TEN with ocular complications.

Citation: Ueta M, Tokunaga K, Sotozono C, Sawai H, Tamiya G, et al. (2012) HLA-A*0206 with TLR3 Polymorphisms Exerts More than Additive Effects in Stevens-Johnson Syndrome with Severe Ocular Surface Complications. PLoS ONE 7(8): e43650. doi:10.1371/journal.pone.0043650

Editor: Yoshihiko Hoshino, National Institute of Infectious Diseases, Japan

Received April 2, 2012; **Accepted** July 24, 2012; **Published** August 17, 2012

Funding: This work was supported in part by grants-in-aid for scientific research from the Japanese Ministry of Health, Labour and Welfare, the Japanese Ministry of Education, Culture, Sports, Science and Technology, a research grant from the Kyoto Foundation for the Promotion of Medical Science, and the Intramural Research Fund of Kyoto Prefectural University of Medicine. The funders had no role in study design, data collection and analysis, decision to publish, or preparation of the manuscript.

Competing Interests: The authors have declared that no competing interests exist.

* E-mail: mueta@koto.kpu-m.ac.jp

Introduction

Stevens-Johnson syndrome (SJS) is an acute inflammatory vesiculobullous reaction of the skin and mucous membranes. It was first described in 1922 by Stevens and Johnson, [1] both pediatricians, who encountered 2 boys aged 8 and 7 who manifested an extraordinary, generalized skin eruption, persistent fever, inflamed buccal mucosa, and severe purulent conjunctivitis resulting in marked visual disturbance. Subsequently, other pediatricians reported that SJS was associated with infectious agents such as *Mycoplasma pneumoniae*, [2] and a viral etiology involving herpes simplex virus, Epstein-Barr virus, cytomegalovirus, and varicella zoster virus [3]. On the other hand, dermatologists claimed that more than 100 different drugs were implicated in eliciting SJS and its severe form, toxic epidermal necrolysis (TEN) [4,5]. The annual incidence of SJS and TEN has been estimated to be 0.4–1 and 1–6 cases per million persons, respectively; [6,7] the reported mortality rate is 3% and 27%, respectively [8]. Although rare, these reactions have high morbidity and mortality rates, and often result in severe and definitive sequelae such as vision loss. SJS/TEN is one of the most devastating ocular surface diseases leading to corneal damage and

loss of vision. The reported incidence of ocular complications in SJS/TEN is 50–68% [7,8].

In the acute stage, patients manifest vesiculobullous lesions of the skin and mucosa, especially that of the eyes and mouth, and severe conjunctivitis. The loss of finger nails in the acute or subacute stage due to paronychia was observed, has been observed in almost all SJS/TEN patients with severe ocular surface complications [9,10,11,12].

In the chronic stage, despite healing of the skin lesions, ocular surface complications such as conjunctival invasion into the cornea [10,11,12,13,14,15,16,17,18]. It is also reported that lid margin keratinization and tarsal scarring, together with lipid tear deficiency, contributes to corneal complications because of blink-related microtrauma [19].

Elsewhere we reported that the frequency of carriers of the HLA-A*0206 antigen is significantly higher among Japanese patients with severe ocular surface complications than in other populations [18,20]. Our single nucleotide polymorphism (SNP) association analysis of candidate genes documented the associated polymorphisms of several immune-related genes including *TLR3*, [12,17] *IL4R*, [14,16] *IL13*, [16] and *FasL* [15]in Japanese SJS/TEN patients with severe ocular surface complications. To elucidate the detailed pathophysiology of SJS/TEN we performed a genome-wide association study of SJS/TEN patients and found associations between 6 SNPs in the prostaglandin E receptor 3 (EP3) gene (*PTGER3*) and SJS/TEN accompanied by severe ocular surface complications [11]. Moreover, gene-gene interaction analysis in SJS/TEN patients with severe ocular surface complications revealed that the interaction between *TLR3* and *PTGER3* exerted SJS/TEN susceptibility effects, and there was a functional interaction between TLR3 and EP3 in a murine experimental allergic conjunctivitis model. [12].

In the present study we examined the multiplicative interaction(s) between HLA-A*0206 and 7 TLR3 SNPs (rs3775296 (uSNP), rs5743312 (iSNP), rs6822014 (gSNP), rs3775290 (sSNP), rs7668666 (iSNP), rs11732384 (iSNP), and rs4861699 (gSNP)) associated with the SJS/TEN patients [12,17] as the onset of SJS/TEN was associated not only with the administration of drugs but also with putative viral syndromes [10,11,12,17]. HLA-A is a component of HLA class I, which resides on the surface of all nucleated cells and alerts the immune system that the cell may be infected by a virus, thereby targeting the cell for destruction. TLR3 recognises viral double-stranded RNA [21].

Results

We analyzed the genotypes for HLA-A and 7 TLR3 SNPs in 110 Japanese SJS/TEN patients with severe ocular complications and 206 healthy volunteers to examine the interactions between the two loci.

We found that HLA-A*0206 exhibited a high odds ratio for SJS/TEN (carrier frequency: $p = 6.9\times10^{-10}$, OR = 5.1; gene frequency: $p = 2.5\times10^{-9}$, OR = 4.0) (Table 1).

We also found that there was a strong association with TLR3 rs.5743312T/T SNP (T/T vs T/C+C/C: $p = 2.5\times10^{-6}$, OR = 7.4), TLR3 rs.3775296T/T SNP (T/T vs T/G+G/G: $p = 8.2\times10^{-6}$, OR = 5.8), TLR3 rs.6822014G/G SNP (G/G vs G/A+A/A: $p = 1.2\times10^{-4}$, OR = 4.8), TLR3 rs.3775290A/A SNP (A/A vs A/G+G/G: $p = 7.1\times10^{-4}$, OR = 2.9), TLR3 rs.7668666A/A SNP (A/A vs A/G+G/G: $p = 1.2\times10^{-3}$, OR = 2.7), TLR3 rs.4861699G/G SNP (G/G vs G/A+A/A:

Table 1. Association between HLA-A*0206 and SJS/TEN with ocular complications.

HLA-A	Carrier frequency				Gene frequency			
	SJS (n = 110)	Normal (n = 206)	p-value (χ^2)	Odds Ratio	SJS (n = 220)	Normal (n = 412)	p-value (χ^2)	Odds Ratio
*0206	46.4% (51/110)	14.6% (30/206)	6.9×10^{-10}	5.07	24.1% (53/220)	7.3% (30/412)	2.5×10^{-9}	4.04
*0101	0% (0/110)	1.4% (3/206)	0.2	–	0% (0/220)	0.7% (3/412)	0.2	–
*0201	26.4% (29/110)	21.4% (44/206)	0.3	–	14.5% (32/220)	11.4% (47/412)	0.3	–
*0207	9.1% (10/110)	7.8% (16/206)	0.7	–	4.5% (10/220)	3.9% (16/412)	0.7	–
*0210	0% (0/110)	1.0% (2/206)	0.3	–	0% (0/220)	0.5% (2/412)	0.3	–
*0301	2.7% (3/110)	1.4% (3/206)	0.4	–	1.4% (3/220)	0.7% (3/412)	0.4	–
*0302	0% (0/110)	0.5% (1/206)	0.5	–	0% (0/220)	0.2% (1/412)	0.5	–
*1101	7.3% (8/110)	18.4% (38/206)	7.3×10^{-3}	0.35	3.6% (8/220)	9.2% (38/412)	1.0×10^{-2}	0.37
*1102	0% (0/110)	0.5% (1/206)	0.5	–	0% (0/220)	0.2% (1/412)	0.5	–
*2402	45.5% (50/110)	60.7% (125/206)	9.5×10^{-3}	0.54	25.0% (55/220)	36.7% (151/412)	2.9×10^{-3}	0.58
*2420	0% (0/110)	0.5% (1/206)	0.5	–	0% (0/220)	0.2% (1/412)	0.5	–
*2601	9.1% (10/110)	12.6% (26/206)	0.3	–	4.5% (10/220)	6.6% (27/412)	0.3	–
*2602	5.5% (6/110)	2.9% (6/206)	0.3	–	2.7% (6/220)	1.7% (7/412)	0.4	–
*2603	1.8% (2/110)	7.8% (16/206)	3.0×10^{-2}	0.2	0.9% (2/220)	3.9% (16/412)	3.2×10^{-2}	0.2
*2605	0% (0/110)	0.5% (1/206)	0.5	–	0% (0/220)	0.2% (1/412)	0.5	–
*2901	0% (0/110)	1.9% (4/206)	0.1	–	0% (0/220)	1.0% (4/412)	0.1	–
*3001	0.9% (1/110)	0% (0/206)	0.2	–	0.5% (1/220)	0% (0/412)	0.2	–
*3101	13.6% (15/110)	16.5% (34/206)	0.5	–	6.8% (15/220)	8.3% (34/412)	0.5	–
*3201	0% (0/110)	0.5% (1/206)	0.5	–	0% (0/220)	0.2% (1/412)	0.5	–
*3303	22.7% (25/110)	14.1% (29/206)	0.05	–	11.4% (25/220)	7.0% (29/412)	0.06	–

doi:10.1371/journal.pone.0043650.t001

Table 2. Association between TLR3 SNPs and SJS/TEN with ocular complications.

rs number of SNP	Genotypes		Case (N = 110)	Control (N = 206)	Allele 1 vs. Allele 2	Genotype 11 vs. 12+22	Genotype 11+12 vs. 22
					P-value[a]	P-value[a]	P-value[a]
					OR[b]	OR[b]	OR[b]
					(95%CI[c])	(95%CI[c])	(95%CI[c])
rs4861699	11	G/G	65/110 (59.1%)	79/206 (38.3%)	0.0016	4.2×10^{-4}	0.28
	12	G/A	36/110 (32.7%)	102/206 (49.5%)	1.80	2.32	1.55
	22	A/A	9/110 (8.2%)	25/206 (12.1%)	(1.25–2.59)	(1.45–3.72)	(0.70–3.45)
rs6822014	11	A/A	55/110 (50.0%)	127/206 (61.7%)	8.9×10^{-4}	0.046	1.2×10^{-4}
	12	A/G	37/110 (33.6%)	71/206 (34.5%)	0.54	0.62	0.21
	22	G/G	18/110 (16.4%)	8/206 (3.9%)	(0.37–0.78)	(0.39–0.99)	(0.09–0.49)
rs11732384	11	G/G	72/110 (65.5%)	103/206 (50.0%)	0.029	0.0085	0.88
	12	G/A	31/110 (28.2%)	89/206 (43.2%)	1.54	1.89	1.07
	22	A/A	7/110 (6.4%)	14/206 (6.8%)	(1.04–2.28)	(1.17–3.06)	(0.42–2.74)
rs3775296	11	G/G	49/110 (44.5%)	109/206 (52.9%)	0.0020	0.16	8.2×10^{-6}
	12	G/T	40/110 (36.4%)	89/206 (43.2%)	0.58	0.71	0.17
	22	T/T	21/110 (19.1%)	8/206 (3.9%)	(0.40–0.82)	(0.45–1.14)	(0.07–0.40)
rs5743312	11	C/C	52/110 (47.3%)	115/206 (55.8%)	0.0014	0.15	2.5×10^{-6}
	12	C/T	38/110 (34.5%)	85/206 (41.3%)	0.56	0.71	0.14
	22	T/T	20/110 (18.2%)	6/206 (2.9%)	(0.39–0.80)	(0.45–1.13)	(0.05–0.35)
rs7668666	11	C/C	36/110 (32.7%)	83/206 (40.3%)	0.0085	0.19	0.0012
	12	C/A	47/110 (42.7%)	101/206 (49.0%)	0.64	0.72	0.37
	22	A/A	27/110 (24.5%)	22/206 (10.7%)	(0.46–0.89)	(0.44–1.17)	(0.20–0.68)
rs3775290	11	G/G	38/110 (34.5%)	82/206 (39.8%)	0.016	0.36	7.1×10^{-4}
	12	G/A	45/110 (40.9%)	103/206 (50.0%)	0.66	0.80	0.35
	22	A/A	27/110 (24.5%)	21/206 (10.2%)	(0.48–0.93)	(0.50–1.29)	(0.18–0.65)

[a]*P*-value for allele or genotype frequency comparisons between cases and controls using the chi-square test.
[b]OR, odds ratio.
[c]CI, confidence interval.
doi:10.1371/journal.pone.0043650.t002

$p = 4.2\times10^{-4}$, OR = 2.3), and TLR3 rs.11732384G/G SNP (G/G vs G/A+A/A: $p = 8.5\times10^{-3}$, OR = 1.9) (Table 2). All SNPs were in Hardy-Weinberg equilibrium ($p>0.01$) in the samples from patients and the controls. Based on the squared correlation coefficient r^2, we investigated the linkage disequilibrium (LD) among the *TLR3* SNPs. We found strong LD between rs.3775296 and rs.5743312 (D' = 1, $r^2 = 0.911$), and between rs.7668666 and rs.3775290 (D' = 0.973, $r^2 = 0.934$) (Fig. 1).

Results of interaction analysis showed that the pair, HLA-A*0206 and TLR3 SNP rs3775296T/T, which exhibited strong LD with TLR3 rs.5743312, exerted more than additive effects. We found that while 11 of the 110 patients (10%) manifested both HLA-A*0206 and TLR3 rs3775296T/T SNP, none of the 206 controls did ($p = 6.5\times10^{-6}$, OR = 47.7, Woolf's correction). The other pairs, HLA-A*0206 and TLR3 rs.3775290A/A SNP, which was in strong LD with TLR3 rs.7668666, or TLR3 rs4861699G/G SNP revealed additive effects: 16 of the 110 patients (14.5%) but only 3 of the 206 controls (1.5%) had both HLA-A*0206 and TLR3 rs.3775290A/A SNP ($p = 7.4\times10^{-6}$, OR = 11.4). In addition, 33 of the 110 patients (30%), compared to 11 of the 206 controls (5.3%), had both HLA-A*0206 and TLR3 rs.4861699G/G SNP ($p = 1.6\times10^{-9}$, OR = 7.6) (Table 3).

Moreover, to examine the interactions within the TLR3 gene alone we analyzed interactions between 2 each of 5 TLR3 SNPs (rs3775296, rs6822014, rs3775290, rs11732384, rs4861699). Combinations of high risk genotypes, on which the observed numbers in cases were greater than of the controls and greater than five, were analyzed. One of the 9 combinations, TLR3 rs6822014G/G and TLR3 rs3775290A/A, exerted more than additive effects (OR 16.1, $p = 2.0\times10^{-6}$) (Table 4). However, the combination HLA-A*0206 and TLR3 rs3775296T/T produced a stronger additive effect than it. In addition, we performed haplotype association analysis with the 7 TLR3 SNPs (rs4861699, rs6822014, rs11732384, rs3775296, rs5743312, rs7668666, rs3775290) and the 5 TLR3 SNPs (rs4861699, rs6822014, rs11732384, rs3775296, rs3775290), and found that no haplotype showed strong association ($p<0.001$) (Table S1). Thus, the haplotype associations appear to contribute little to the observed interactions.

Discussion

To our knowledge, ours is the first report documenting the additive effects of HLA-A*0206 and TLR3 polymorphisms. Our interaction analysis showed that the pair HLA-A*0206 and TLR3 SNP rs3775296T/T, which was in strong LD with TLR3 rs.5743312, exerted more than additive effects, and that other pairs, HLA-A*0206 and TLR3 rs.3775290A/A SNP in strong LD

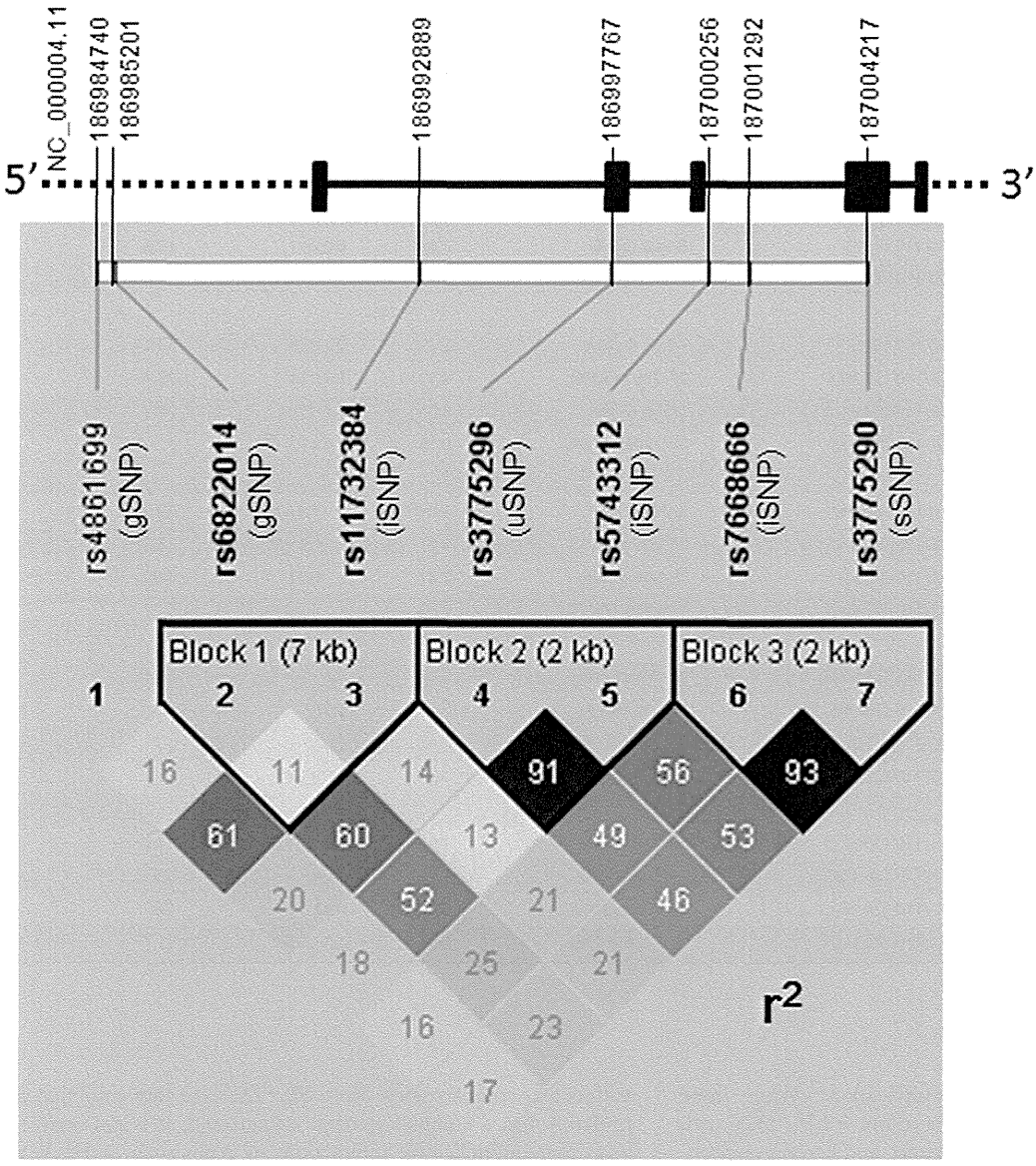

Figure 1. Linkage disequilibria among the 7 *TLR3* SNPs. Strong linkage disequilibrium was observed between rs.3775296 and rs.5743312, and between rs.7668666 and rs.3775290.
doi:10.1371/journal.pone.0043650.g001

with TLR3 rs.7668666, and TLR3 rs4861699G/G SNP exerted additive effects. Moreover, the combination HLA-A*0206 and TLR3 rs3775296T/T was stronger than the combination with TLR3 rs6822014G/G or TLR3 rs3775290A/A, the interactions within the TLR3 gene alone.

HLA-A, a component of HLA class I, alerts the immune system that the cell may be infected with a virus; TLR3 recognizes viral double-stranded RNA [21]. It is worth noting that about 80% of our SJS patients developed SJS after receiving treatment for the common cold with antibiotics, cold remedies, and/or NSAIDs; only about 5% of our SJS patient progressed to SJS after drug treatment to prevent the occurrence of convulsions [11,12]. Moreover, our review of medical records revealed that 9 of the 11 patients with both HLA-A*0206 and TLR3 SNP rs3775296T/T (and rs.5743312T/T) developed SJS after receiving cold medicine, leading us to suspect that they already had a viral infection before taking the cold medicine. Particulars on the other 2 patients are unknown because they developed SJS during childhood.

Although the TLR3 SNPs exerting additive- or more than additive effects with HLA-A*0206 were u-, i-, or gSNPs and without amino acid changes, it is possible that TLR3 SNPs and HLA-A*0206 were involved in the onset of SJS with severe ocular surface complications. Moreover, their interaction might influence the host immune response against viral infection with drug treatments.

Earlier reports indicated regional differences in HLA associations. Although in Japanese SJS patients we were unable to detect the HLA-Bw44 antigen, a subgroup of HLA-B12 [19,23], it was significantly increased in Caucasian SJS patients with ocular involvement [22].

On the other hand, the HLA-A*0206 antigen, which is not found in Caucasians [18,19] was significantly increased in our

Table 3. Interaction analysis between HLA-A*0206 and various TLR3 SNPs.

HLA-A*0206	TLR3 SNP	SJS patients (N = 110)	Controls (N = 206)	OR	p-value	Standardized OR
HLA-A*0206 & TLR3 rs3775296 T/T						
+	+	11/110 (10%)	0/206 (0%)	47.7*	6.5×10^{-6}**	262.7
+	−	40/110 (36.4%)	30/206 (14.6%)	3.4	8.8×10^{-6}	18.5
−	+	10/110 (9.1%)	8/206 (3.9%)	2.5	0.057	13.6
−	−	49/110 (44.5%)	168/206 (81.6%)	0.18	1.4×10^{-11}	1
HLA-A*0206 & TLR3 rs6822014G/G						
+	+	8/110 (7.3%)	3/206 (1.5%)	5.3**	0.019**	32.3
+	−	43/110 (39.1%)	27/206 (13.1%)	4.3	1.2×10^{-7}	25.9
−	+	10/110 (9.1%)	5/206 (2.4%)	4.0**	0.012**	24.5
−	−	49/110 (44.5%)	171/206 (83.0%)	0.16	1.4×10^{-12}	1
HLA A*0206 & TLR3 rs3775290A/A						
+	+	16/110 (14.5%)	3/206 (1.5%)	11.4**	7.4×10^{-6}**	49.0
+	−	35/110 (31.8%)	27/206 (13.1%)	3.1	6.6×10^{-5}	13.2
−	+	11/110 (10%)	18/206 (8.7%)	1.2	0.71	4.9
−	−	48/110 (43.6%)	158/206 (76.7%)	0.24	4.2×10^{-9}	1
HLA A*0206 & TLR3 rs11732384G/G						
+	+	37/110 (33.6%)	16/206 (7.8%)	6.0	4.5×10^{-9}	16.4
+	−	14/110 (12.7%)	14/206 (6.8%)	2	0.077	5.5
−	+	35/110 (31.8%)	87/206 (42.2%)	0.64	0.070	1.7
−	−	24/110 (21.8%)	89/206 (43.2%)	0.37	1.5×10^{-4}	1
HLA A*0206 & TLR3 rs4861699 G/G						
+	+	33/110 (30%)	11/206 (5.3%)	7.6	1.6×10^{-9}	25.7
+	−	18/110 (16.4%)	19/206 (9.2%)	1.9	0.060	6.5
−	+	32/110 (29.1%)	68/206 (33.0%)	0.83	0.48	2.8
−	−	27/110 (24.5%)	108/206 (52.4%)	0.30	1.8×10^{-6}	1

*Woolf's correction,
**Fisher's exact test.
doi:10.1371/journal.pone.0043650.t003

Japanese SJS patients with ocular complications. While there might be ethnic differences in the association of SJS/TEN with HLA,[18,19] specific combinations of genes and certain environmental factors may be required for the manifestation of this rare phenotype. [10,11,12,18,19].

Elsewhere [12] we reported that the epistatic interaction between TLR3 and PTGER3 confers an increased risk for SJS with ocular complications. Since SJS/TEN is a rare condition that probably has a complex genetic background, it is reasonable to posit that multiplicative interactions of genes such as HLA-A & TLR3, and TLR3 & PTGER3, are required for the phenotypic manifestation.

In summary, we show that HLA-A*0206 with TLR3 polymorphisms exerts more than additive effects in SJS with severe

Table 4. Interaction analysis of two SNPs of the TLR3 SNPs (SJS > control and SJS >5).

Combination of 2 TLR3 SNPs		SJS (N = 110)	Controls (N = 206)	OR	p-value
rs3775296 T/T +	rs3775290 A/A +	19/110 (17.3%)	6/206 (2.9%)	7.0	6.6×10^{-6}
rs11732384 G/G +	rs3775290 A/A +	27/110 (24.5%)	21/206 (10.2%)	2.9	7.1×10^{-4}
rs6822014 G/G +	rs3775290 A/A +	15/110 (13.6%)	2/206 (1.0%)	16.1	2.0×10^{-6}
rs4861699 G/G +	rs3775290 A/A +	26/110 (23.6%)	16/206 (7.8%)	3.7	7.5×10^{-5}
rs11732384 G/G +	rs3775296 T/T +	21/110 (19.1%)	8/206 (3.9%)	5.8	8.2×10^{-6}
rs6822014 G/G +	rs3775296 T/T +	17/110 (15.5%)	4/206 (1.9%)	9.2	4.3×10^{-6}
rs4861699 G/G +	rs3775296 T/T +	21/110 (19.1%)	8/206 (3.9%)	5.8	8.2×10^{-6}
rs6822014 G/G +	rs11732384 G/G +	18/110 (16.4%)	8/206 (3.9%)	4.8	1.2×10^{-4}
rs4861699 G/G +	rs6822014 G/G +	18/110 (16.4%)	8/206 (3.9%)	4.8	1.2×10^{-4}

doi:10.1371/journal.pone.0043650.t004

ocular surface complications and we suggest that gene-gene interactions should be considered in addition to major single-locus effects.

Materials and Methods

Patients

This study was approved by the institutional review board of Kyoto Prefectural University of Medicine and the University of Tokyo, Graduate School of Medicine. All experimental procedures were conducted in accordance with the principles of the Helsinki Declaration. The purpose of the research and the experimental protocols were explained to all participants, and their prior written informed consent was obtained.

Diagnosis of SJS/TEN was based on a confirmed history of acute onset of high fever, serious mucocutaneous illness with skin eruptions, and involvement of at least 2 mucosal sites including the ocular surface [9,11,12,17,18].

To investigate the gene-gene interaction between HLA-A*0206 and TLR3, we enrolled 110 SJS/TEN patients in the chronic or subacute phase; all presented with symptoms of ocular surface complications. None of the patients were relatives. The controls were 206 healthy volunteers. All participants and volunteers were Japanese residing in Japan. The average age of the 110 patients and 206 controls was 43.6±18.0 (SD) and 35.4±11.1 (SD) years, respectively. The male:female ratios in the patient and control groups were 42:68 and 82:124, respectively. Some of the SJS/TEN patients and controls in this study were subjects in our earlier reports [12,17,18,19].

TLR3 SNPs Genotyping

Genomic DNA was isolated from human peripheral blood at SRL Inc. (Tokyo, Japan). Genotyping for 2 SNPs of TLR3 (rs3775290, 3775296) was performed by PCR-direct sequencing as reported previously [17]. For direct sequencing, PCR amplification was conducted with AmpliTaq Gold DNA Polymerase (Applied Biosystems) for 35 cycles at 94°C for 1 min, annealing at 60°C for 1 min, and 72°C for 1 min on a commercial PCR machine (GeneAmp; Perkin-Elmer Applied Biosystems). The PCR products were reacted with BigDye Terminator v3.1 (Applied Biosystems) and sequence reactions were resolved on an ABI PRISM 3100 Genetic Analyzer (Applied Biosystems).

Genotyping for 5 SNPs of TLR3 (rs4861699, rs6822014, rs11732384, rs5743312, rs7668666) as performed using DigiTag2 assay [12]. Multiplex PCR was performed in 10 μl of Multiplex PCR buffer containing 25 ng genomic DNA, 25 nM of each multiplex primer mix, 200 μM of each dNTP, 2.25 mM $MgCl_2$, and 0.4 U KAPA2G Fast HotStart DNA polymerase (Kapa Biosystems). Cycling was performed at 95°C for 3 min, followed by 40 cycles of 95°C for 15 s and 68°C for 2 min. The primers and probes used in this study previously were reported [12,17].

HLA-A Genotyping

For HLA-A genotyping, we performed polymerase chain reaction amplification followed by hybridization with sequence-specific oligonucleotide probes (PCR-SSO) using commercial bead-based typing kits (WAK Flow, Wakunaga, Hiroshima, Japan), as described previously [18,19].

Statistical Analysis

Statistical significance of the association with each SNP was assessed using Chi-square test or Fisher's exact test on two-by-two contingency tables. When the value obtained for the control was 0 the odds ratio was calculated using Woolf's correction.

Haploview software (ver. 4.2) was used to infer the linkage disequilibrium structure of the 7 TLR3 SNPs and to perform a haplotype analysis of TLR3 gene.

Supporting Information

Table S1 Haplotype analysis of TLR3 gene. Haplotype association analysis with the 7 TLR3 SNPs (rs4861699, rs6822014, rs11732384, rs3775296, rs5743312, rs7668666, rs3775290) and the 5 TLR3 SNPs (rs4861699, rs6822014, rs11732384, rs3775296, rs3775290)
(DOCX)

Author Contributions

Conceived and designed the experiments: MU. Performed the experiments: MU KT HS. Analyzed the data: MU KT HS GT. Contributed reagents/materials/analysis tools: MU CS TI SK. Wrote the paper: MU.

References

1. Stevens AM, Johnson FC (1922) A new eruptive fever associated with stomatitis and opthalmia: report of two cases in children. Am J Dis Child 24: 526–533.
2. Leaute-Labreze C, Lamireau T, Chawki D, Maleville J, Taieb A (2000) Diagnosis, classification, and management of erythema multiforme and Stevens-Johnson syndrome. Arch Dis Child 83: 347–352.
3. Forman R, Koren G, Shear NH (2002) Erythema multiforme, Stevens-Johnson syndrome and toxic epidermal necrolysis in children: a review of 10 years' experience. Drug Saf 25: 965–972.
4. Roujeau JC, Kelly JP, Naldi L, Rzany B, Stern RS, et al. (1995) Medication use and the risk of Stevens-Johnson syndrome or toxic epidermal necrolysis. N Engl J Med 333: 1600–1607.
5. Wolf R, Orion E, Marcos B, Matz H (2005) Life-threatening acute adverse cutaneous drug reactions. Clin Dermatol 23: 171–181.
6. Auquier-Dunant A, Mockenhaupt M, Naldi L, Correia O, Schroder W, et al. (2002) Correlations between clinical patterns and causes of erythema multiforme majus, Stevens-Johnson syndrome, and toxic epidermal necrolysis: results of an international prospective study. Arch Dermatol 138: 1019–1024.
7. Yetiv JZ, Bianchine JR, Owen JA Jr. (1980) Etiologic factors of the Stevens-Johnson syndrome. South Med J 73: 599–602.
8. Power WJ, Ghoraishi M, Merayo-Lloves J, Neves RA, Foster CS (1995) Analysis of the acute ophthalmic manifestations of the erythema multiforme/Stevens-Johnson syndrome/toxic epidermal necrolysis disease spectrum. Ophthalmology 102: 1669–1676.
9. Sotozono C, Ueta M, Koizumi N, Inatomi T, Shirakata Y, et al. (2009) Diagnosis and treatment of Stevens-Johnson syndrome and toxic epidermal necrolysis with ocular complications. Ophthalmology 116: 685–690.
10. Ueta M, Kinoshita S (2010) Innate immunity of the ocular surface. Brain Res Bull 81: 219–228.
11. Ueta M, Sotozono C, Nakano M, Taniguchi T, Yagi T, et al. (2010) Association between prostaglandin E receptor 3 polymorphisms and Stevens-Johnson syndrome identified by means of a genome-wide association study. J Allergy Clin Immunol 126: 1218–1225 e1210.
12. Ueta M, Tamiya G, Tokunaga K, Sotozono C, Ueki M, et al. (in press) Epistatic interaction between TLR3 and PTGER3 confers an increased risk for Stevens-Johnson syndrome with ocular complications. J Allergy Clin Immunol.
13. Sotozono C, Ang LP, Koizumi N, Higashihara H, Ueta M, et al. (2007) New grading system for the evaluation of chronic ocular manifestations in patients with Stevens-Johnson syndrome. Ophthalmology 114: 1294–1302.
14. Ueta M, Sotozono C, Inatomi T, Kojima K, Hamuro J, et al. (2007) Association of IL4R polymorphisms with Stevens-Johnson syndrome. J Allergy Clin Immunol 120: 1457–1459.
15. Ueta M, Sotozono C, Inatomi T, Kojima K, Hamuro J, et al. (2008) Association of Fas Ligand gene polymorphism with Stevens-Johnson syndrome. Br J Ophthalmol 92: 989–991.
16. Ueta M, Sotozono C, Inatomi T, Kojima K, Hamuro J, et al. (2008) Association of combined IL-13/IL-4R signaling pathway gene polymorphism with Stevens-Johnson syndrome accompanied by ocular surface complications. Invest Ophthalmol Vis Sci 49: 1809–1813.

17. Ueta M, Sotozono C, Inatomi T, Kojima K, Tashiro K, et al. (2007) Toll-like receptor 3 gene polymorphisms in Japanese patients with Stevens-Johnson syndrome. Br J Ophthalmol 91: 962–965.
18. Ueta M, Sotozono C, Tokunaga K, Yabe T, Kinoshita S (2007) Strong Association Between HLA-A*0206 and Stevens-Johnson Syndrome in the Japanese. Am J Ophthalmol 143: 367–368.
19. Ueta M, Tokunaga K, Sotozono C, Inatomi T, Yabe T, et al. (2008) HLA class I and II gene polymorphisms in Stevens-Johnson syndrome with ocular complications in Japanese. Mol Vis 14: 550–555.
20. Di Pascuale MA, Espana EM, Liu DT, Kawakita T, Li W, Gao YY, et al. (2005) Correlation of corneal complications with eyelid cicatricial pathologies in patients with Stevens-Johnson syndrome and toxic epidermal necrolysis syndrome. Ophthalmology. 112: 904–912.
21. Kawai T, Akira S (2007) TLR signaling. Semin Immunol 19: 24–32.
22. Mondino BJ, Brown SI, Biglan AW (1982) HLA antigens in Stevens-Johnson syndrome with ocular involvement. Arch Ophthalmol 100: 1453–1454.
23. Kaniwa N, Saito Y, Aihara M, Matsunaga K, Tohkin M, et al. (2010) HLA-B*1511 is a risk factor for carbamazepine-induced Stevens-Johnson syndrome and toxic epidermal necrolysis in Japanese patients. Epilepsia 51: 2461–2465.

The Relation Between Visual Performance and Clinical Ocular Manifestations in Stevens-Johnson Syndrome

MINAKO KAIDO, MASAKAZU YAMADA, CHIE SOTOZONO, SHIGERU KINOSHITA, JUN SHIMAZAKI, YOSHITSUGU TAGAWA, YUKO HARA, TAIICHIRO CHIKAMA, AND KAZUO TSUBOTA

• PURPOSE: To investigate the relation between visual function, clinical findings, and visual symptoms in Stevens-Johnson syndrome (SJS) and to compare the results with Sjögren syndrome (SS) patients and normal subjects.

• DESIGN: Cross-sectional comparative study.

• METHODS: One hundred fifteen eyes of 59 consecutive patients with SJS and toxic epidermal necrolysis (TEN), 208 eyes of 104 healthy normal subjects, and 132 eyes of 66 SS patients were investigated in this multicenter study. All study subjects underwent tear function and ocular surface examinations, Landolt and functional visual acuity examinations, and the Japanese version of the NEI VFQ-25 (National Eye Institute Visual Function Questionnaire).

• RESULTS: The mean ocular surface grading scores were significantly higher and the mean score of all 12 NEI VFQ subscales was significantly lower in the SJS patients compared to the SS patients and the normal subjects ($P < .05$). The conventional and functional logarithm of minimal angle of resolution (logMAR) visual acuities in SJS patients with minimal corneal complications were significantly higher and the mean total composite NEI VFQ scores were lower compared to SS patients. The conventional and functional logMAR visual acuities and the mean ocular surface grading scores in SJS with aqueous deficiency were significantly higher and the mean total composite NEI VFQ scores were lower compared to SS patients. Strong correlations between best-corrected logMAR functional visual acuities and either ocular surface grading scores or the composite NEI VFQ-25 scores were observed.

• CONCLUSIONS: The functional visual acuity examination reflects the severity of clinical ocular surface findings and vision-related quality of life more than the standard conventional visual acuity in SJS. (Am J Ophthalmol 2012;154:499–511. © 2012 by Elsevier Inc. All rights reserved.)

Accepted for publication Mar 28, 2012.

From the Department of Ophthalmology, Keio University School of Medicine, Tokyo, Japan (M.K., K.T.); Department of Ophthalmology, Tokyo Medical Center, Tokyo, Japan (M.Y.); Department of Ophthalmology, Kyoto Prefectural University of Medicine, Kyoto, Japan (C.S., S.K.); Department of Ophthalmology, Tokyo Dental College, Ichikawa, Japan (J.S.); Department of Ophthalmology, Hokkaido University School of Medicine, Hokkaido, Japan (Y.T.); Department of Ophthalmology, Ehime University School of Medicine, Ehime, Japan (Y.H.); and Department of Ophthalmology, Yamaguchi University Graduate School of Medicine, Yamaguchi, Japan (T.C.).

Inquiries to Minako Kaido, Department of Ophthalmology, Keio University School of Medicine, Shinanomachi 35, Shinjuku-ku, Tokyo, 160-8582, Japan; e-mail: fwiw1193@mb.infoweb.ne.jp

STEVENS-JOHNSON SYNDROME (SJS) IS AN ACUTE, self-limiting disease of the skin and mucous membranes associated with symblepharon, adhesive occlusion of the lacrimal puncta, and corneal opacification with conjunctivalization and severe dry eyes leading to worsening of the ocular surface health and poor quality of vision.[1–8]

Previous reports have demonstrated that contrast sensitivity, contrast visual acuity, glare disability, and wavefront aberrations are useful to detect quality of vision in everyday life.[9–19] Visual function assessment using these measurement methods has been reported to be useful in keratorefractive surgery, mild cataract, and dry eye diseases.[9–19] To the best of our knowledge, however, there are no reports about visual function assessment in patients with SJS except a previously published report by us.[8]

It has been our experience that SJS patients with good visual acuity and mild ocular surface morbidity may still complain of similar severe eye irritation and visual complaints as patients with Sjögren syndrome (SS). However, the differences in visual symptoms and conventional and dynamic visual acuity between these 2 entities have not been quantified and compared so far. In an attempt to investigate the visual function and ocular surface differences between SJS and SS, we performed this multicenter cross-sectional study, using a previously reported ocular surface morbidity severity questionnaire and functional visual acuity measurement.[20–24]

METHODS

• SUBJECTS: One hundred fifteen eyes of 59 consecutive patients (28 male, 31 female; mean age: 47.5 ± 16.0 years; range: 14–79 years) with SJS, including its more severe variant, toxic epidermal necrolysis (TEN), seen at the Cornea Subspecialty Outpatient Clinic of the Departments of Ophthalmology of Keio University, Tokyo Dental College, Tokyo Medical Center, Kyoto Prefectural University of Medicine, Hokkaido University, Ehime University, and Yamaguchi University were studied in this cross-sectional multicenter study. Clinicians participating

0002-9394/$36.00
http://dx.doi.org/10.1016/j.ajo.2012.03.044

TABLE 1. Clinical Severity Grading Criteria of the Ocular Surface Findings

	Grade 0	Grade 1	Grade 2	Grade 3	Comments
Assessment of Corneal Complications					
SPK	A1D1	A1D2, A2D1	A1D3, A2D2, A3D1	A2D3, A3D2, A3D3	Using fluorescein staining based on the area and density of the lesions as described by Miyata and associates[29]
Corneal epithelial defect	Absent	Less than 1/4 of the corneal surface	1/4 to 1/2 of the corneal surface	More than 1/2 of the corneal surface	
Conjunctivalization	Absent	Less than 1/4 of the corneal surface	1/4 to 1/2 of the corneal surface	More than 1/2 of the corneal surface	
Neovascularization	Absent	Confined to the corneal periphery	Extending beyond the pupil margin	Extending beyond the pupil margin into the central cornea	In eyes where significant opacification or extensive symblepharon formation made it difficult to evaluate corneal neovascularization, a grade of 3 was assigned
Corneal opacification	Clear cornea with easily visible iris details	Partial obscuration of the iris details	Iris details poorly seen with barely visible pupil margins	Complete obscuration of iris and pupil details	
Keratinization	Absent	Less than 1/4 of the corneal surface	1/4 to 1/2 of the corneal surface	More than 1/2 of the corneal surface	
Assessment of Conjunctival Complications					
Conjunctival hyperemia	Absent	Mild or sectoral engorgement of the conjunctival vessels	Moderate or diffuse engorgement of the conjunctival vessels	Severe or significant engorgement of the conjunctival vessels	
Symblepharon	Absent	Involving only the conjunctival surface	Less than 1/2 of the corneal surface	More than 1/2 of the corneal surface	
Assessment of Eyelid Complications					
Trichiasis	Absent	Less than 1/4 of the lid margin	1/4 to 1/2 of the lid margin	More than 1/2 of the lid margin	

Continued on next page

TABLE 1. Clinical Severity Grading Criteria of the Ocular Surface Findings *(Continued)*

MJ involvement	Normal MJ	Mild irregularity of MJ	Moderate irregularity of MJ	Severe irregularity of MJ	Bron grading was employed for the classification of MJ changes.[30] Fluorescein staining of the conjunctiva was performed for evaluating the MJ involvement. In eyes where significant keratinization of the lid margin or extensive symblepharon formation made it difficult to evaluate mucocutaneous junction involvement, Grade 3 was assigned.
MG involvement	Oily expressible secretion	Expressible yellowish-white oily secretion	Expressible thick cheesy material	Inability to express any secretion	The severity was determined clinically by the nature of the meibomian gland secretion expressed manually at the center of the upper lid.
Punctal involvement	Normal	Iatrogenic punctal occlusion	Either superior or inferior punctal occlusion	Both superior and inferior punctal occlusion	

A = area; D = density; MG = mucocutaneous gland; MJ = mucocutaneous junction; SPK = superficial punctuate keratopathy.

in the study received training to standardize the conduct of examinations performed at each center. The conduct of examinations was checked by trained coordinators at each center for consistency of the examination procedures. The diagnosis of SJS or TEN was based on the history of the presence of cryptogenic fever and acute inflammation of mucosal membranes most commonly after taking cold remedies, antibiotics, or anti-inflammatory drugs, and on the presence of chronic ocular surface complications such as symblepharon, entropion, trichiasis, xerophthalmia, and/or corneal vascularization.[1,3–5] Two hundred eight eyes of 104 healthy normal subjects (30 male, 74 female; mean age: 36.2 ± 12.0 years; range: 20–72 years) without dry eye disease and 132 eyes of 66 SS patients (66 female; mean age: 62.8 ± 11.1 years; range: 28–82 years) who were diagnosed according to Fox criteria were also investigated in this multicenter study.[25] Patients or control subjects with other systemic or ocular diseases, history of ocular surgery within 6 months, history of ocular cicatricial pemphigoid, or chemical, thermal, or radiation injury that would have adverse ocular surface effects were excluded according to the study exclusion criteria. SJS patients with a baseline best-corrected Landolt conventional visual acuity of less than 20/2000 attributable to cataract in both eyes, ocular surface keratinization, glaucoma, or posterior segment disease were excluded from this study, since the functional visual acuity measurement system cannot assess functional visual acuity at such low visual acuity levels.

• **SLIT-LAMP EXAMINATIONS:** All study subjects underwent slit-lamp examinations observing 12 components of 3 categories of ocular complications, such as corneal complications consisting of superficial punctuate keratopathy (SPK), epithelial defect, conjunctivalization, neovascularization, opacification, and keratinization; conjunctival complications consisting of hyperemia and symblepharon formation; and eyelid complications consisting of trichiasis, mucocutaneous junction involvement, meibomian gland involvement, and punctal damage. Each component was graded on a scale from 0 to 3, depending on the severity of involvement.[26]

The severity gradings and ocular surface tests were performed under the same single protocol by the researchers of all contributing study centers. Table 1 shows the clinical severity grading criteria of the ocular surface findings.

• **TEAR FUNCTION AND OCULAR SURFACE EXAMINATIONS:** The standard Schirmer test without topical anesthesia was performed as previously reported.[7] A vital staining severity grading was also assigned. A 2-μL volume of 1% fluorescein dye was instilled in the conjunctival sac by a micropipette. The minimum score for corneal fluorescein staining was 0 points and the maximum score was 9 points.[27]

• **STANDARD VISUAL ACUITY MEASUREMENTS:** Standard visual acuity testing using Landolt charts placed 5 m away from subjects was performed. Landolt visual acuity

TABLE 2. Standard Visual Acuity and Visual Parameters Assessed by Functional Visual Acuity Measurement System in Eyes of Patients With Sjögren Syndrome, Stevens-Johnson Syndrome Patients, and Healthy Normal Subjects

	SJS	SS	Normal
Conventional visual acuity			
logMAR	0.76 ± 0.76	−0.004 ± 0.13	−0.10 ± 0.10
Decimal	0.17	1.01	1.26
Functional visual acuity			
logMAR	0.98 ± 0.62[a]	0.28 ± 0.27[a]	−0.008 ± 0.13
Decimal	0.10	0.52	1.02
Maximal visual acuity			
logMAR	0.83 ± 0.65	0.10 ± 0.26	−0.15 ± 0.12
Decimal	0.15	0.79	1.41
Minimal visual acuity			
logMAR	1.19 ± 0.60	0.53 ± 0.36	0.17 ± 0.19
Decimal	0.06	0.30	0.68
Visual maintenance ratio	0.86 ± 0.12	0.91 ± 0.07[b]	0.98 ± 0.05[c,d]
Reaction time	1.0 ± 0.2	1.1 ± 0.2	1.0 ± 0.2
Blink number	11.2 ± 9.3	17.2 ± 9.6[b]	16.4 ± 8.7[c]

logMAR = logarithm of minimal angle of resolution; logMAR = logarithm of minimal angle of resolution; SJS = Stevens-Johnson syndrome; SS = Sjögren syndrome; VA = visual acuity.

[a] $P < .05$ between conventinal VA and functional VA.

[b] $P < .05$ between groups of SJS and SS.

[c] $P < .05$ between groups of SJS and Normal.

[d] $P < .05$ between groups of SS and Normal.

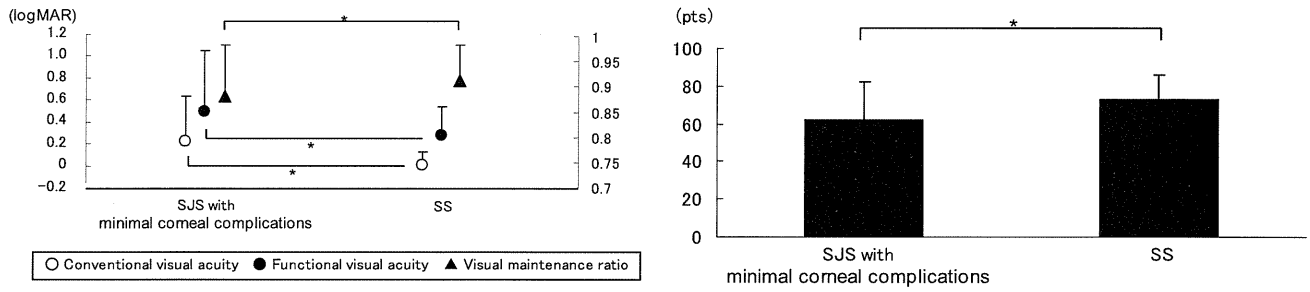

FIGURE 1. Visual function and Visual Function Questionnaire-25 in Stevens-Johnson syndrome (SJS) with minimal corneal complications and Sjögren syndrome (SS) patients. (Left) Conventional and functional visual acuity and visual maintenance ratio in Stevens-Johnson syndrome with minimal corneal complications and Sjögren syndrome patients. (Right) Total composite NEI VFQ-25 scores in Stevens-Johnson syndrome with minimal corneal complications and Sjögren syndrome patients. logMAR = logarithm of minimal angle of resolution.

was employed instead of Snellen chart since it is a standard test in Japan, and because the optotypes in Landolt and functional visual acuity testing are similar.

• FUNCTIONAL VISUAL ACUITY MEASUREMENTS: Continuous visual acuity testing during a 60-second period under natural blinking was performed as previously reported.[24]

• FUNCTIONAL VISUAL ACUITY INDICES: Briefly, the outcome parameters of the functional visual acuity measurement system were functional visual acuity (defined as the average of visual acuities measured during a 60-second testing), visual maintenance ratio (defined as the ratio of logMAR values of the functional visual acuities over the time frame for testing divided by the logarithm of minimal angle of resolution (logMAR) baseline visual acuity),[7] maximal corrected visual acuity, minimal corrected visual acuity, standard deviation of functional visual acuity, mean reaction time (defined as the mean of the response time taken by a subject to respond to an optotype), and blink numbers during a 60-second functional visual acuity test.

• VISUAL FUNCTION QUESTIONNAIRE-25: We used the Japanese version of the NEI VFQ-25 (National Eye Insti-